Hidden sectors at FCC-*ee* with two-particle angular correlations

E. Musumeci[1], A. Irles[1], R. Perez-Ramos[2,3], I. Corredoira[4], E. Sarkisyan-Grinbaum[5,6], V. A. Mitsou[a)][1], M. A. Sanchis-Lozano[1]

[1] *IFIC, CSIC and Universitat de València, C/ Catedrático José Beltrán 2, 46980 Paterna, Spain*
[2] *DRII-IPSA, 63 bis Boulevard de Brandebourg, 94200 Ivry-sur-Seine, France*
[3] *Laboratoire de Physique Théorique et Hautes Energies (LPTHE), UMR 7589, Sorbonne Université et CNRS, 4 place Jussieu, 75252 Paris Cedex 05, France*
[4] *Instituto Galego de Física de Altas Enerxìas (IGFAE, USC), Spain*
[5] *Experimental Physics Department, CERN, 1211 Geneva 23, Switzerland*
[6] *Department of Physics, The University of Texas at Arlington, Arlington, TX 76019, USA*

Future e^+e^- colliders are called to play a fundamental role in measuring Standard Model (SM) parameters with unprecedented precision and the discovery of physics beyond the SM (BSM). This study focus on a QCD-like Hidden Valley (HV) scenario, with relatively light v-quarks, perturbing the QCD partonic cascade and modifying azimuthal and (pseudo)-rapidity correlations of final-state SM hadrons. We assume a collision energy of 240 GeV and we consider an ILD-for-FCC detector to study unexpected structures arising in the two-particle angular correlation function, including selection cuts and detector effects.

This work is submitted to the FCC Feasibility Study in preparation for the European Strategy for Particle Physics Update 2025.

[a] Corresponding author

1 Introduction

Correlations play a fundamental role in the study of hadronic dynamics since the beginning of cosmic ray and accelerator physics [1, 2]. The study of angular correlations has revealed new phenomena in heavy-ion collisions, later also found in simpler collisions (proton–proton, proton–nucleus) [3–5]

In particular, long-range near-side ridges show up in two-particle angular correlations, while different theoretical explanations have been put forward to understand this initially unexpected phenomenon [6–11]. Almost all of them require the existence of some unconventional state of matter at the primary interaction of the collision (like quark-gluon plasma), ultimately yielding collective effects among final-state SM particles. On the other hand, no clear ridge-like signal was found in the e^+e^- data analysed by ALEPH [12] and Belle [13] experiments, except for recent claims [14] at the highest available energy and high multiplicity of ALEPH archival data.

Motivated by such unexpected correlation structures found in high-energy collisions, we have looked at possible *anomalies* in both azimuthal and (pseudo)rapidity correlations to obtain a useful insight into an unknown stage of matter on top of the QCD parton shower. We focus on two-particle angular correlations as a way of searching for BSM at future high-energy e^+e^- colliders, as they provide a much cleaner environment than hadron colliders. In previous works, we have considered e^+e^- collisions in the International Linear Collider (ILC), at particle level [15] and including detector effects [16] simulating the performance of the ILD experiment.

The theoretical framework of New Physics (NP) here is based on the so-called *Hidden Valley* (HV) scenario, which stands for a wide class of models with one or more hidden sectors beyond the SM. Thereby, new (valley) particles of mass $\lesssim 100$ GeV arise, still surviving all present discovery limits.

2 Two-particle angular correlations

The clean environment of e^+e^- collisions, in contrast to hadronic collisions, is especially suitable to define a reference frame whose z-axis lies along the direction of the back-to-back jets in most events. The thrust reference frame has been used throughout this work, so the rapidity y of a particle always refers to the thrust- or z-axis. The azimuthal angle ϕ is defined as usual on the transverse plane to the thrust axis, event by event. Note that only rapidity and azimuthal differences of two final-state SM charged particles labelled as '1' and '2', $\Delta y \equiv y_1 - y_2$, $\Delta\phi \equiv \phi_1 - \phi_2$, are used.

The two-particle correlation function is defined as

$$C^{(2)}(\Delta y, \Delta\phi) = \frac{S(\Delta y, \Delta\phi)}{B(\Delta y, \Delta\phi)}, \tag{1}$$

where $S(\Delta y, \Delta\phi)$ stands for the density of particle pairs within the same event

$$S(\Delta y, \Delta\phi) = \frac{1}{N_{\text{pairs}}} \frac{d^2 N^{\text{same}}}{d\Delta y d\Delta\phi}, \tag{2}$$

while $B(\Delta y, \Delta\phi)$ represents the density of mixed particle pairs from distinct events

$$B(\Delta y, \Delta\phi) = \frac{1}{N_{\text{mix}}} \frac{d^2 N^{\text{mix}}}{d\Delta y d\Delta\phi}. \tag{3}$$

The azimuthal yield, $Y(\Delta\phi)$, is of particular interest, being defined by integration over a given Δy range as:

$$Y(\Delta\phi) = \frac{\int_{y_{\text{inf}} \le |\Delta y| \le y_{\text{sup}}} S(\Delta y, \Delta\phi) dy}{\int_{y_{\text{inf}} \le |\Delta y| \le y_{\text{sup}}} B(\Delta y, \Delta\phi) dy}, \tag{4}$$

where $y_{\text{inf/sup}}$ defines the lower/upper integration limit for different rapidity intervals.

3 HV phenomenology

In most HV models [17], the SM gauge group sector G_{SM} is extended by (at least) a new gauge group G_{V} under which all SM particles are neutral. Hence, a new category of *v-particles* emerges charged under G_{V}, but neutral under G_{SM}. Moreover, "communicators", charged under both G_{SM} and G_{V}, are introduced to the theory allowing interactions between SM and HV particles. Communicators can be either intermediate (very massive) vector Z_v bosons, or hidden partners of SM quarks or leptons, generically denoted as F_v, assumed to be pair produced. In this study, F_v are taken as spin-1/2 fermions and q_v as spin-0 scalars.

Different mechanisms can connect the hidden and SM sectors through communicators, e.g., via the tree-level channel: $e^+e^- \to Z_v \to q_v\bar{q}_v \to$ hadrons. Alternatively, communicators can be pair produced via SM γ^*/Z coupling to a $F_v\bar{F}_v$ pair, yielding both visible and invisible cascades in the same event. We have confirmed that the latter channel significantly dominates over the former in the collision energy under study.

For some values of the HV parameter space, communicators can *promptly* decay into a particle f of the visible sector (its SM partner) and a q_v of the hidden sector according to the splitting: $F_v \to f q_v$. Note that the q_v mass may strongly influence the kinematics of the visible cascade (leading to SM particles) in the same event, thereby yielding observational consequences. This mass remains currently unconstrained ranging from zero to close to the F_v mass [18], so different values are probed in our analysis.

We study the effect of the invisible (HV) sector on the partonic cascade into final-state SM particles, leading to potentially observable angular correlations. This can be understood, e.g., as both visible and hidden cascades have to share the event's total energy, thereby modifying their respective available phase spaces, as depicted in Fig. 1(a) for a HV cascade and in Fig. 1(b) for SM initiated by $q\bar{q}$. We restrict our study to a QCD-like HV scenario with q_v-quarks, g_v-gluons, and an equivalent "strong" coupling constant α_v. For simplicity, α_v is assumed not running with energy but fixed to $\alpha_v = 0.1$, as no significant differences were found in our analysis by varying this value.

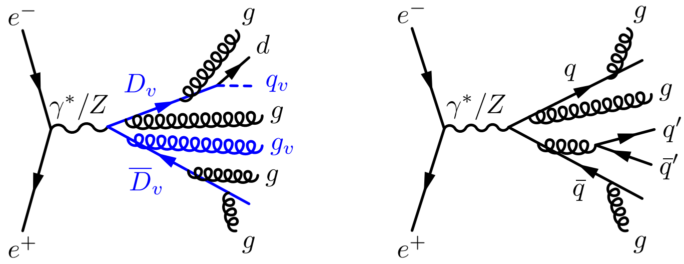

(a) Hidden valley (b) SM light quarks

Figure 1: Leading diagrams of production in e^+e^- collisions for (a) HV, and (b) SM light quarks including bottom.

4 Analysis at detector level with ILD-for-FCC

To assess the feasibility of HV signal detection in FCC-e^+e^-, we have used the PYTHIA8 Monte Carlo event generator [19] both for signal and background production, as the HV particles and interactions are already implemented. Fast detector simulations were carried out using the SGV tool [20] with the geometry and acceptance modelled after the *ILD-for-FCC*, which is an adaptation of the ILD concept [21] for the FCC-e^+e^-. The simulated event format is the one used by the ILD concept group and the event reconstruction and analysis is based on the ILCSOFT package. The reconstructed candidates of single particles are called Particle Flow Objects (PFOs). In our study, we consider a centre-of-mass energy, $\sqrt{s}$, of e^+e^- collisions equal to 240 GeV, which corresponds to the FCC-e^+e^- running phase of the ZH maximum production [22] as a Higgs boson factory. Â¡

The HV signal proceeds via the process $e^+e^- \to D_v\bar{D}_v \to$ hadrons, where D_v denotes the lightest communicator, being the hidden partner of the d-quark, as depicted in Fig. 1(a). In our benchmark scenarios we set $\alpha_v = 0.1$ and $m_{D_v} = 120$ GeV $= \sqrt{s}/2$, with three different v-quark mass values: $m_{q_v} = 10$ and 100 GeV. We also consider $m_{D_v} = 100$ GeV and with $m_{q_v} = 50$ GeV to test the sensitivity dependence on m_{D_v}.

At $\sqrt{s} = 240$ GeV, the $e^+e^- \to q\bar{q}$ background comes from the inclusive production of all the SM quark species except the top flavour, since its production lies below threshold (see Fig. 1). Here, we also consider the background coming from Initial State Radiation (ISR), unlike a previous preliminary study [15]. Four-fermion production (dominated by $e^+e^- \to WW$) was neither considered earlier but its contribution (included here) has been found to be negligible. The cross-sections for the HV and SM processes have been estimated with PYTHIA8 reported in Table 1.

In view of the small cross-sections for HV production from Table 1, specific cuts have to be implemented to maximise the background removal while keeping the signal as much as possible. On the other hand, displaced vertices due to the production and decay of long-lived particles have not been considered here as we are focusing on prompt decays of v-particles and their effect on the partonic cascade yielding final-state SM

Table 1: Cross-sections for $e^+e^- \to D_v\bar{D}_v$, $e^+e^- \to q\bar{q}$ and $WW \to 4q$ processes at $\sqrt{s} = 240$ GeV, with different assumptions for the m_{D_v} and m_{q_v} masses. Efficiencies of the selection criteria described in the main text, average charged-track multiplicities and their RMS, are shown.

Process		σ_{PYTHIA8} [pb]	Efficiency [%]	$\langle N_{\text{ch}}\rangle$
$e^+e^- \to D_v\bar{D}_v$				
m_{D_v} [GeV]	m_{q_v} [GeV]			
120	100	0.129	40.2	5.6±1.9
120	10	0.136	6.4	5.6±1.9
100	50	1.32	1.7	7.0±2.3
$e^+e^- \to q\bar{q}$ with ISR			0.12	5.5±2.1
$WW \to 4q$		1.54	0.17	13.7±3.5

particles. Following a strategy similar to that in [23], constraints have been set on the number of neutral PFOs and charged ones (≤ 22 and ≤ 15, respectively). Other cuts were applied to the emission angle ($|\cos\theta_{\gamma_{\text{ISR}}}| < 0.5$) and energy ($E_{\gamma_{\text{ISR}}} < 40$ GeV) of reconstructed ISR photons. Constraints on the di-jet invariant mass m_{jj} have also been defined, accepting values below 130 GeV. Furthermore, an energy upper limit of 80 GeV was implemented to the leading jet.

The selection-cut efficiency, reported in Table 1, shows a drastic reduction of the SM background while the HV signal is affected to a much lesser extent. For the computation of B, only a thrust value larger than 0.95 was imposed, keeping the same requirements on PFO multiplicities as for S.

Figure 2 presents three-dimensional plots of the two-particle correlation function $C^{(2)}(\Delta y, \Delta\phi)$ separately for the HV and the SM scenarios, before (Fig. 2(a)) and after (Fig. 2(b)) cuts. As an example, in the HV case we set $m_{q_v} = 100$ GeV, $m_{D_v} = 120$ GeV and $\alpha_v = 0.1$ alongside the decay $D_v \to d + q_v$ initiating the partonic (both visible and invisible) shower. As expected, a near-side peak shows up at ($\Delta y \simeq 0, \Delta\phi \simeq 0$), receiving contributions mainly from track pairs within the same jet. On the other hand, an away-side correlation ridge around $\Delta\phi \simeq \pi$, and extending over a large rapidity range, results from back-to-back momentum balance, in principle unrelated to NP effects. After cuts, a near-side ridge (with two pronounced and symmetric bumps) shows up for $1.6 < |\Delta y| < 3$ at $\Delta\phi \simeq 0$ for the SM case, similar to the pure HV scenario. This structure arises from the ISR effect, since the effective centre-of-mass energy approaches the Z mass, and thus resonant production greatly enhances the production cross-section. It becomes of paramount importance to take this effect into account in our analysis, mimicking possible HV signatures in angular correlations.

In order to examine in more detail the possibility of discriminating the HV signal from the pure SM background, we depict in Fig. 3 the yield $Y(\Delta\phi)$ (defined in Eq. (4)) for both $0 < |\Delta y| \leq 1.6$ and $1.6 < |\Delta y| < 5$ ranges: before (Fig. 3(a)) and after (Fig. 3(b)) cuts. The HV signal for various masses m_{D_v}, m_{q_v} is considered together with the SM

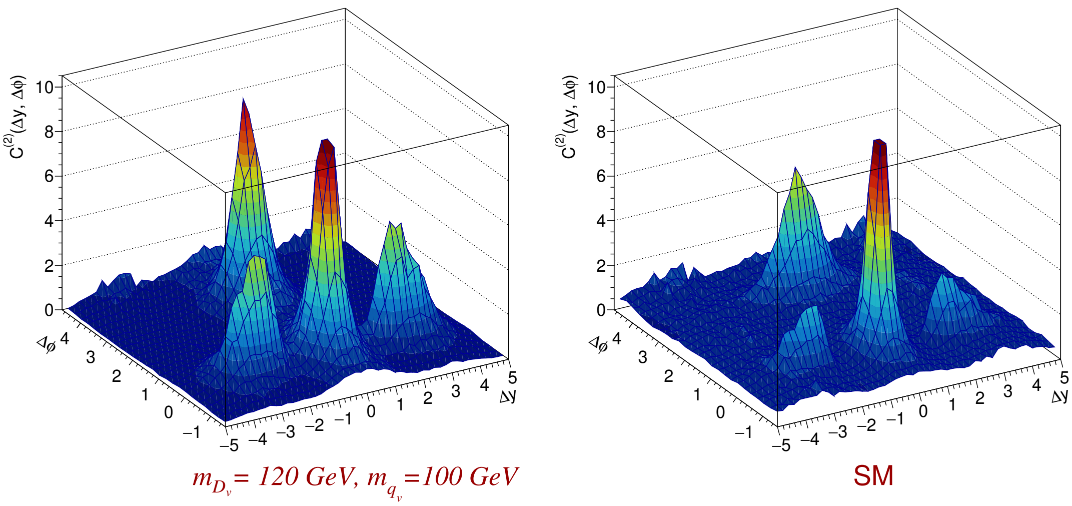

(a) Detector level distributions with no selection applied to the $S(\Delta y, \Delta\phi)$ reconstruction.

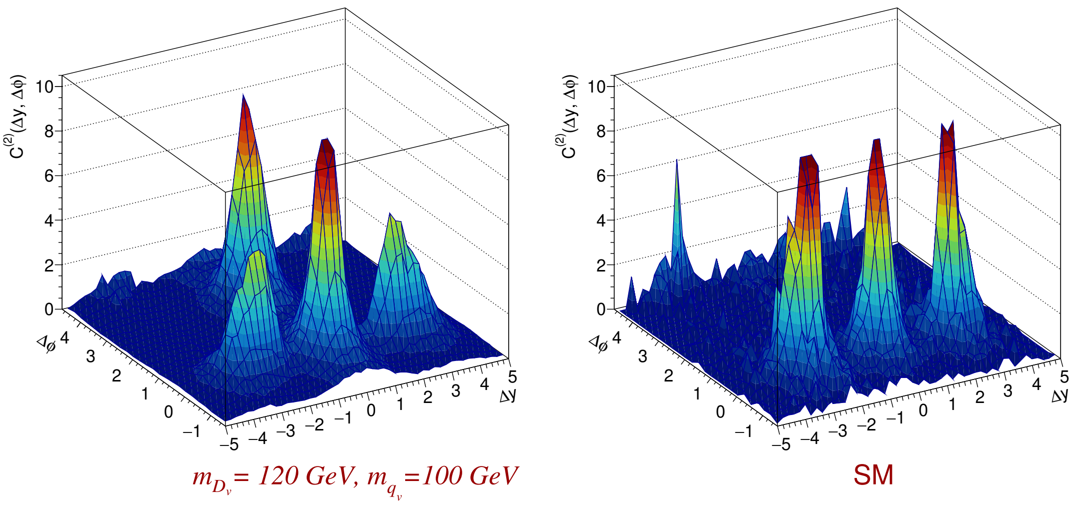

(b) Detector level distributions after the signal enriching experimental cuts applied to the $S(\Delta y, \Delta\phi)$ reconstruction.

Figure 2: 3D plots of the two-particle angular correlation function, $C^{(2)}(\Delta y, \Delta\phi)$, at detector level, separately for the pure HV signal and the SM background in e^+e^- collisions at $\sqrt{s} = 240$ GeV. In the pure HV case, $m_{q_v} = 100$ GeV, $m_{D_v} = 120$ GeV and $\alpha_v = 0.1$ were set. For the SM case, light quarks include the bottom flavour.

background, while a standalone analysis of the SM background is also presented. A clear difference becomes apparent for $0 < |\Delta y| \leq 1.6$: a sizeable peak at $\Delta\phi \sim \pi$ characterises the HV scenario, unlike the pure SM case. This remarkable discrepancy of

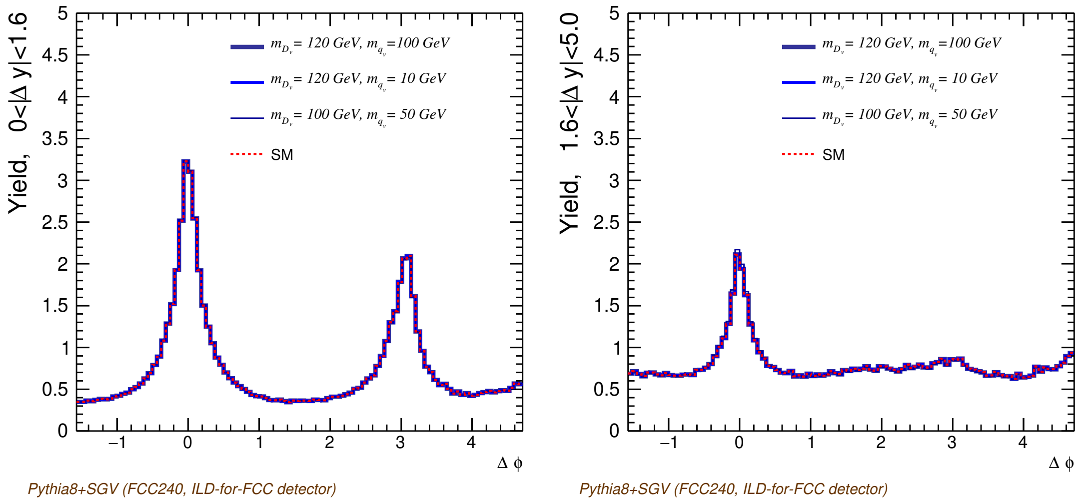

(a) Detector-level yield distributions with no selection cuts applied.

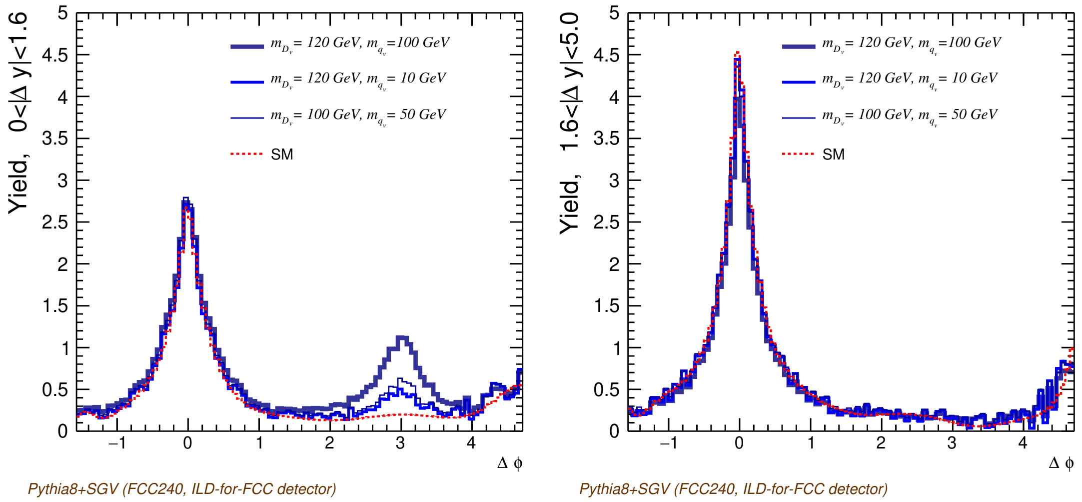

(b) Detector-level yield distributions after the selection cuts were applied to enrich the $S(\Delta y, \Delta\phi)$ sample with HV signal events.

Figure 3: Yield $Y(\Delta\phi)$ for both HV signal in association with SM and for pure SM background (red line) for the $0 < |\Delta y| < 1.6$ (left) and $1.6 < |\Delta y| < 5$ intervals (right), respectively. Notice the different shapes of the HV+SM signal and SM background resulting after applying the selection cuts, providing a valuable signature of NP using angular correlations.

shapes would potentially serve as a valuable signature of a hidden sector, complementary to more conventional BSM searches.

5 Conclusions

The results show that two-particle azimuthal correlations in the FCC-e^+e^- Higgs factory can become a useful tool to discover NP if kinematically accessible, as postulated in Refs. [24, 25]. Although a specific HV model has been employed here, other types of hidden sectors could yield similar signatures. In addition, collective effects stemming from a source different from BSM cannot be excluded in this kind of analysis. Such searches, based on rather diffuse signals that spread over a large number of final-state particles, should be contemplated as complementary to other more conventional methods, thereby increasing the discovery potential of these machines.

Acknowledgements

We acknowledge M. Berggren and the ILD software working group for their support with the usage of detector fast simulation and the reconstruction tools employed in this study. AI, EM and VAM acknowledge support by the Spanish MCIU/ AEI / 10.13039/501100011033 and the European Union / FEDER through the grant PID2021-122134NB-C21. EM and VAM acknowledge support by Generalitat Valenciana (GV) via the Excellence Grant CIPROM/2021/073. AI acknowledges support by GV under the grant number CIDEGENT/2020/21, the financial support from the MCIN with funding from the European Union NextGenerationEU and by GV via the Programa de Planes Complementarios de I+D+i (PRTR 2022) Project *Si4HiggsFactories*, reference ASFAE/2022/015. IC acknowledges support by the Xunta de Galicia (CIGUS Network of Research Centers). MASL acknowledges support by the Spanish Agencia Estatal de Investigacion under grant PID2020-113334GB-I00 / AEI / 10.13039/501100011033, and by GV under grant CIPROM/2022/36.

References

[1] W. Kittel, E. A. De Wolf, *Soft multihadron dynamics*, World Scientific, 2005, ISBN: 978-981-4480-54-3, DOI: 10.1142/5805.

[2] R. Botet, M. Ploszajczak, *Universal fluctuations: The phenomenology of hadronic matter*, World Scientific, 2002, ISBN: 978-981-4488-95-2, DOI: 10.1142/4916.

[3] CMS, V. Khachatryan et al., *Measurement of long-range near-side two-particle angular correlations in pp collisions at* $\sqrt{s}$ *=13 TeV*, Phys. Rev. Lett. **116** (2016) 172302, DOI: 10.1103/PhysRevLett.116.172302, arXiv: 1510.03068 [nucl-ex].

[4] ALICE, B. Abelev et al., *Long-range angular correlations on the near and away side in p-Pb collisions at* $\sqrt{s_{NN}} = 5.02$ *TeV*, Phys. Lett. B **719** (2013) 29, DOI: 10.1016/j.physletb.2013.01.012, arXiv: 1212.2001 [nucl-ex].

[5] ATLAS, G. Aad et al.,
Observation of Associated Near-Side and Away-Side Long-Range Correlations in $\sqrt{s_{NN}} = 5.02$ *TeV Proton-Lead Collisions with the ATLAS Detector*,
Phys. Rev. Lett. **110** (2013) 182302, DOI: 10.1103/PhysRevLett.110.182302,
arXiv: 1212.5198 [hep-ex].

[6] E. V. Shuryak,
On the origin of the 'Ridge' phenomenon induced by jets in heavy ion collisions,
Phys. Rev. C **76** (2007) 047901, DOI: 10.1103/PhysRevC.76.047901,
arXiv: 0706.3531 [nucl-th].

[7] A. Dumitru, F. Gelis, L. McLerran, R. Venugopalan,
Glasma flux tubes and the near side ridge phenomenon at RHIC,
Nucl. Phys. A **810** (2008) 91, DOI: 10.1016/j.nuclphysa.2008.06.012,
arXiv: 0804.3858 [hep-ph].

[8] P. Bozek, W. Broniowski,
Collective dynamics in high-energy proton-nucleus collisions,
Phys. Rev. C **88** (2013) 014903, DOI: 10.1103/PhysRevC.88.014903,
arXiv: 1304.3044 [nucl-th].

[9] M.-A. Sanchis-Lozano, E. Sarkisyan-Grinbaum,
A correlated-cluster model and the ridge phenomenon in hadron–hadron collisions,
Phys. Lett. B **766** (2017) 170, DOI: 10.1016/j.physletb.2017.01.001,
arXiv: 1610.06408 [hep-ph].

[10] M.-A. Sanchis-Lozano, E. Sarkisyan-Grinbaum,
Ridge effect and three-particle correlations, Phys. Rev. D **96** (2017) 074012,
DOI: 10.1103/PhysRevD.96.074012, arXiv: 1706.05231 [hep-ph].

[11] J. Noronha, B. Schenke, C. Shen, W. Zhao,
Progress and Challenges in Small Systems, 2024, arXiv: 2401.09208 [nucl-th].

[12] A. Badea, A. Baty, P. Chang, G. M. Innocenti, M. Maggi, C. Mcginn, M. Peters, T.-A. Sheng, J. Thaler, Y.-J. Lee, *Measurements of two-particle correlations in* e^+e^- *collisions at 91 GeV with ALEPH archived data*, Phys. Rev. Lett. **123** (2019) 212002,
DOI: 10.1103/PhysRevLett.123.212002, arXiv: 1906.00489 [hep-ex].

[13] Belle, Y. C. Chen et al.,
Measurement of Two-Particle Correlations of Hadrons in e^+e^- *Collisions at Belle*,
Phys. Rev. Lett. **128** (2022) 142005, DOI: 10.1103/PhysRevLett.128.142005,
arXiv: 2201.01694 [hep-ex].

[14] Y.-C. Chen et al., *Long-range near-side correlation in e+e− collisions at 183-209 GeV with ALEPH archived data*, Phys. Lett. B **856** (2024) 138957,
DOI: 10.1016/j.physletb.2024.138957, arXiv: 2312.05084 [hep-ex].

[15] E. Musumeci, R. Perez-Ramos, A. Irles, I. Corredoira, V. A. Mitsou, E. Sarkisyan-Grinbaum, M. A. Sanchis-Lozano, *Two-particle angular correlations in the search for new physics at future e^+e^- colliders*, International Workshop on Future Linear Colliders, 2023, arXiv: 2307.14734 [hep-ph].

[16] E. Musumeci, A. Irles, R. Perez-Ramos, I. Corredoira, E. Sarkisyan-Grinbaum, V. A. Mitsou, M. A. Sanchis-Lozano, *Exploring hidden sectors with two-particle angular correlations at future e^+e^- colliders* (2023), arXiv: 2312.06526 [hep-ph].

[17] M. J. Strassler, K. M. Zurek, *Echoes of a hidden valley at hadron colliders*, Phys. Lett. B **651** (2007) 374, DOI: 10.1016/j.physletb.2007.06.055, arXiv: hep-ph/0604261.

[18] R. Pérez-Ramos, M.-A. Sanchis-Lozano, E. K. Sarkisyan-Grinbaum, *Searching for hidden matter with long-range angular correlations at e^+e^- colliders*, Phys. Rev. D **105** (5 2022) 053001, DOI: 10.1103/PhysRevD.105.053001, arXiv: 2110.05900 [hep-ph].

[19] T. Sjöstrand, S. Ask, J. R. Christiansen, R. Corke, N. Desai, P. Ilten, S. Mrenna, S. Prestel, C. O. Rasmussen, P. Z. Skands, *An introduction to PYTHIA 8.2*, Comput. Phys. Commun. **191** (2015) 159, DOI: 10.1016/j.cpc.2015.01.024, arXiv: 1410.3012 [hep-ph].

[20] M. Berggren, *SGV 3.0 – a fast detector simulation* (2012), arXiv: 1203.0217 [physics.ins-det].

[21] ILD Concept Group, H. Abramowicz et al., *International Large Detector: Interim Design Report* (2020), arXiv: 2003.01116 [physics.ins-det].

[22] FCC, *Future Circular Collider (FCC) Feasibility Study Midterm Report*, tech. rep., CERN/SPC/1218/RA, CERN/FC/6734/RA, 2024.

[23] A. Irles, J. P. Márquez, R. Pöschl, F. Richard, A. Saibel, H. Yamamoto, N. Yamatsu, *Probing gauge-Higgs unification models at the ILC with quark–antiquark forward–backward asymmetry at center-of-mass energies above the Z mass*, Eur. Phys. J. C **84** (2024) 537, DOI: 10.1140/epjc/s10052-024-12918-z, arXiv: 2403.09144 [hep-ph].

[24] M.-A. Sanchis-Lozano, *Prospects of searching for (un)particles from Hidden Sectors using rapidity correlations in multiparticle production at the LHC*, Int. J. Mod. Phys. A **24** (2009) 4529, DOI: 10.1142/S0217751X09045820, arXiv: 0812.2397 [hep-ph].

[25] M.-A. Sanchis-Lozano, E. K. Sarkisyan-Grinbaum, *Searching for new physics with three-particle correlations in pp collisions at the LHC*, Phys. Lett. B **781** (2018) 505, DOI: 10.1016/j.physletb.2018.04.033, arXiv: 1802.06703 [hep-ph].